Scanning pentaprism measurements of off-axis aspherics

Peng Su[a], James H. Burge[a,b], Brian Cuerden[b], Jose Sasian[a], Hubert M. Martin[b]

[a]College of Optical Sciences, the Univ. of Arizona, Tucson, AZ 85721-0094
[b]Dept. of Astronomy/Steward Observatory, the Univ. of Arizona, Tucson, AZ 85721-0065

ABSTRACT

The pentaprism test is based on the property of a paraboloidal surface where all rays parallel to the optical axis will go through its focal point. We have developed a scanning pentaprism system that exploits this geometry to measure off-axis paraboloidal mirrors such as those for the Giant Magellan Telescope primary mirror. Extension of the pentaprism test to off-axis mirrors requires special attention to field effects that can be ignored in the measurement of an axisymmetric mirror. The test was demonstrated on a 1. -m diameter off-axis mirror and proved to have about 50nm rms surface accuracy. This paper gives detailed performance results for the measurement of the 1.7 m mirror, and designs and analysis for the test of the GMT segments.

Keywords: Aspherics, telescope, optical testing

1. INTRODUCTION

The scanning pentaprism test has been an important absolute test method for flat mirrors, for parabolic mirrors and also for collimation systems.[1,2] During a measurement, a pentaprism is used to relay a collimated beam from an autocollimator or a beam projector to the surface under test. The angle of the reflected beam is a measure of the surface slope of the mirror. The pentaprism is scanned across the surface to sample the slope error at a number of points. The powerful advantage of using a pentaprism is that it deviates light by a fixed angle (nominally 90 degrees) regardless of the orientation of the pentaprism to the incident beam. Thus, the resulting measurements are relatively insensitive to the prism movement errors or alignment errors.

We are building a scanning pentaprism test for the 8.4 m off-axis segments of the Giant Magellan Telescope (GMT).[3] This test will be used to measure low-order aberrations (through spherical aberration and trefoil) and will serve as a validation of the principal optical test, which is a full-aperture interferometric test with a large, non-axisymmetric null corrector.[4] For a paraboloidal surface, the pentaprism test is a null test in that, for a perfect mirror, the reflected light comes to focus at a point that does not move as the pentaprism is scanned across the surface. The GMT primary mirror is nearly a paraboloid, with a conic constant of -0.9983, so a small systematic spot motion is desired.

We built a prototype of the scanning pentaprism system and used it to measure the 1.7 m off-axis primary mirror of the New Solar Telescope (NST) at Big Bear Solar Observatory, whose surface is nearly a 1/5 scale model of a GMT segment. Since rotational symmetry is broken for the off-axis surface, there are a number of special considerations for the pentaprism test, relative to its use for a flat or axisymmetric mirror.

In this paper, the principles and the implementation of the scanning pentaprism test are described, as developed for testing an off-axis parabolic mirror. The paper also gives detailed performance results for the measurement of the NST mirror, and designs and analysis for the test of the GMT segments.

2. SYSTEM DESIGN AND ANALYSIS

2.1 Basic principle

An ideal parabolic mirror will focus on-axis parallel rays to a point at the focus. One can measure errors in the surface by sending parallel rays into the mirror and measuring where they intercept the focal plane. The scanning pentaprism system uses a collimated light source and a pentaprism to create parallel beams that are scanned over the surface, as shown in Fig. 1. For an off-axis mirror, several scans across different diameters are used to determine the low-order

aberrations in the system. We used four pentaprism scans to test the NST mirror. The measurement of spot position in the image plane as a function of pupil position gives a complete measurement of the low-order surface errors.
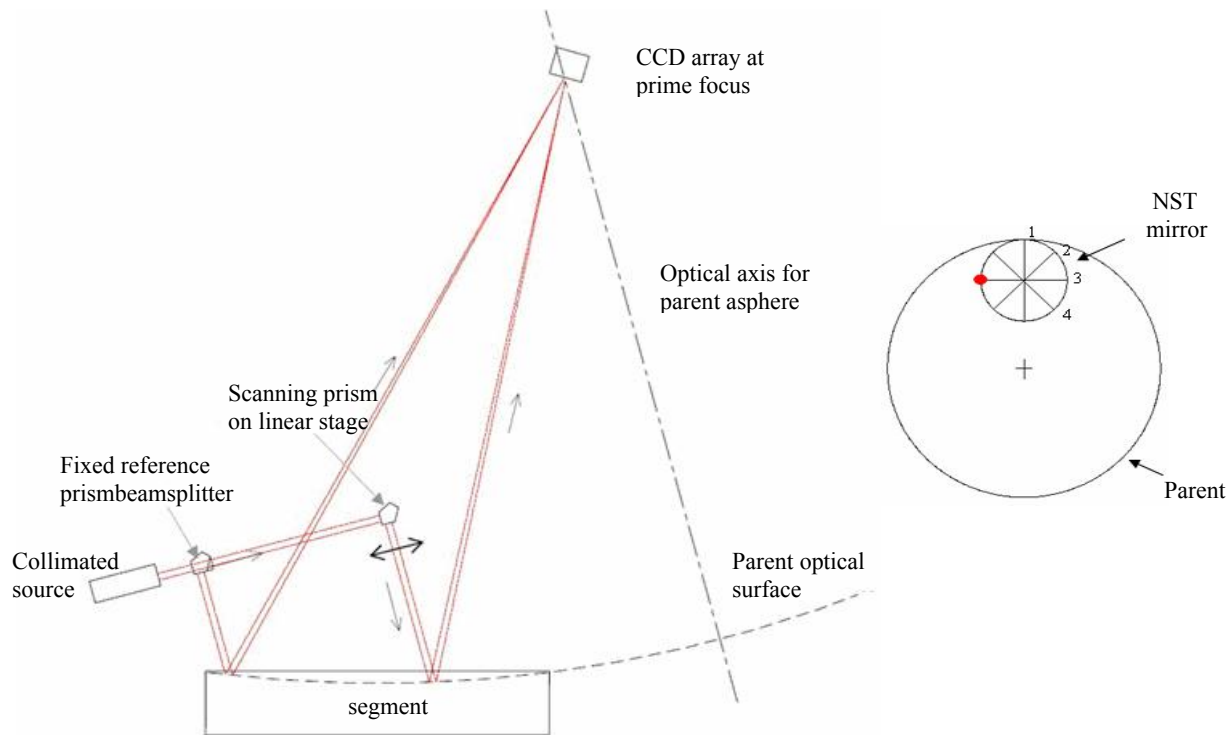

Fig.1. Basic principle of the scanning pentaprism test, illustrated for the NST mirror

Variations in tilt of the collimated source, or beam projector, also cause spot motion. We remove this error by using a stationary pentaprism-beamsplitter in addition to the scanning pentaprism. Common motion of both spots is due to changes in the beam projector, while the differential motion is a measure of the slope error at the pupil position of the scanning beam.

2.2 Prism properties

The pentaprism test works because the deflection of the beam is independent of rotation of the pentaprism about an axis defined by the intersection of its entrance and exit faces. This is the pitch direction indicated in Fig. 2. The corresponding direction on the mirror surface and in the focal plane is called the in-scan direction, and the perpendicular direction is the cross-scan direction. The scanning pentaprism system measures slope errors in the in-scan direction with high accuracy. Rotation of the prism about its other axes (roll and yaw) causes first-order deflection of the beam in the cross-scan direction, so we use the cross-scan information only as a guide to align the system, not as a measurement of surface slopes.

The only first-order source of in-scan spot motion is a change in pitch of the beam projector, and this is removed by the differential measurement with two pentaprisms. There are second-order effects, however, that must be considered. Table 1 lists sources of line-of-sight error, to second order. Prism yaw will introduce quadratic motions in the in-scan direction, and yaw of the beam projector couples with prism rotations to cause in-scan motion. Finally, there is uncertainty in determining the in-scan direction in the focal plane. This error is called detector roll in the table. An error of $\Delta\theta$ in determining the in-scan direction will cause a coupling of cross-scan motion into the in-scan measurement. This can be expressed as (in-scan error) = (cross-scan motion) $\times \Delta\theta$.

Table 1. Contributions to line-of-sight error from prism, beam projector, and determination of in-scan direction

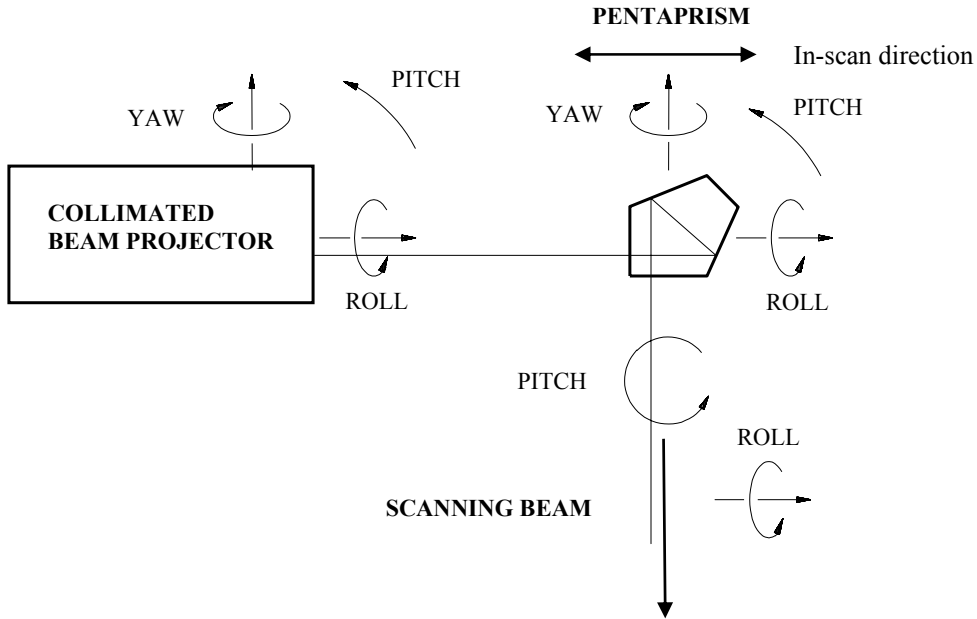| Contributions to in-scan motion	Contributions to cross-scan motion
Beam projector pitch	Beam projector yaw
(Prism yaw)^2	Prism yaw
(Prism yaw) x (beam projector yaw)	Prism roll
(Prism roll) x (beam projector yaw)	(Prism roll) x (beam projector pitch)
(Detector roll) x (cross-scan motion)	(Prism yaw) x (beam projector pitch)

Fig.2. Definition of degrees of freedom for scanning pentaprism

To minimize the second order effects from prism yaw and roll, we use an electronic autocollimator to monitor yaw of the scanning prism, and correct it with a pico-motor actuator on the prism. We then use another actuator to correct roll of the prism, using the cross-scan spot motion as feedback.

2.3 Field effects

If the paraboloidal mirror is illuminated with collimated light that is parallel to its axis, all reflected rays go through the focal point. If these rays are not parallel to the axis, the rays will shift away from the focal point and they no longer intersect at a point. For a full axially symmetric mirror, this effect is described as Seidel coma. The off-axis segment covers part of the comatic pattern, which appears as a combination of astigmatism and coma in the wavefront. The magnitude of this aberration is linear with the misalignment.

The pentaprism test for an off-axis paraboloid has some special characteristics when compared with the test for a rotationally symmetric surface. As shown in the right of Fig. 1, only one of the four scans is in the plane containing the optical axis of the parent. Plane symmetry is not available for scans 2, 3 and 4. Moreover, as an off-axis part of a parabolic surface, the mirror suffers field aberrations. For the case of the NST mirror, there is a 2.3:1 ratio between the image location (chief ray) shift and the coma blur in the tangential direction. Spot displacement caused by field aberration is not small relative to the shift of the chief ray.

Because of the two features mentioned above, the in-scan and cross-scan directions of the test in the detector plane are no longer perpendicular to each other but instead change orientation at different pupil locations during a single scan. An intuitive way to understand this is shown in Fig. 3. A cross-scan motion would introduce a field angle. The figure shows that as the field changes linearly with pentaprism roll and yaw, the pattern of the field error is linearly shifted and scaled. Connecting the spots from the same position on the mirror surface with lines, one can see that the in-scan and cross-scan directions in the focal plane are changing at different positions of the mirror due to the field aberration.
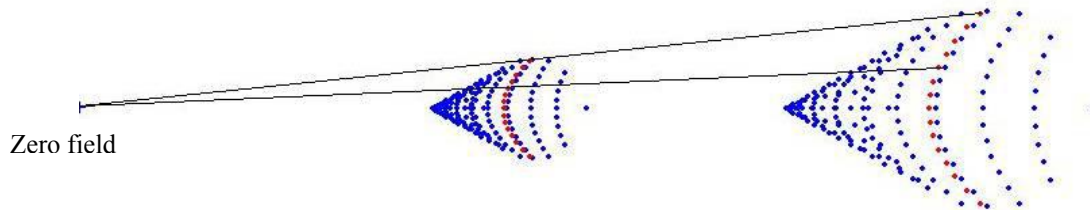

Zero field

Fig.3. Changes in field angle will linearly shift and scale the spot diagram. The cross-scan direction depends on pupil position.

Since the in-scan and cross-scan directions change with respect to pupil position, we measure these directions at discrete sampling positions and interpolate to find the directions for other positions. We determine the cross-scan direction by rolling the prism with its roll actuator. The in-scan direction is defined as the perpendicular direction.

3. DEMONSTRATION FOR A 1.7 M OFF-AXIS PARABOLOID

3.1 System layout

The NST primary mirror is a 1.7 m diameter off-axis paraboloid with a 1.84 m off-axis distance to the center of the mirror. The vertex radius of curvature of its parent is 7.7 m. The scanning pentaprism assembly for the NST mirror, shown in Fig. 4, uses two pentaprisms on a rail. A collimated light source projects light along the rail. The stationary pentaprism-beamsplitter is located at one end of the rail near the beam projector. The scanning pentaprism can be positioned at any point along the rail using motor control. A detector is located at the focal point to capture spot images.
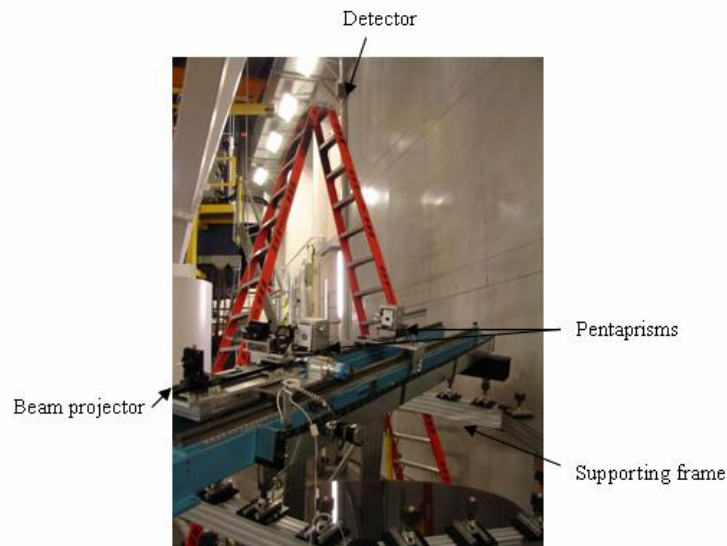

Fig.4. Scanning pentaprism layout

3.2 Data collection and reduction procedure

A pentaprism scan consists of 20-40 samples across a diameter of the mirror. A full measurement consists of four or more scans across different diameters. For each scan, the scanning pentaprism is driven by a motor to sample different positions on the mirror. Spot images are recorded after the prism yaw and roll corrections are performed. We use a correlation method to find the centers of the spots from the two prisms. The spot displacements are then projected to the in-scan direction, and the displacement of the stationary prism's spot is subtracted from that of the scanning prism. The spot displacements are divided by the focal length to obtain the wavefront slopes.

We use the pentaprism data to determine a set of low-order aberrations. We fit Zernike polynomials to the slopes from all scans to obtain the wavefront error of the system. We control the relative field angles of the different scans by measuring a single common point at the center of the mirror in all scans. A non-zero field angle produces a combination of coma and astigmatism, so we can determine the field angle from the fitted aberrations. If the field aberrations are large enough to affect the measurement of low-order figure errors, we can realign the system and repeat the measurement.

During data collection, we use a laser tracker to monitor the position of the mirror and the detector. We can use this information to add corrections to each scan.

Because we only sample 20-40 points across each diameter, surface errors with high spatial frequency can be aliased into the low-order aberrations that we determine from the pentaprism data. We have accurate measurements of small-scale figure errors from the interferometric optical test, so we can subtract these small-scale slopes from the pentaprism data.

Fig. 5 gives the flow diagram for data collection and processing.
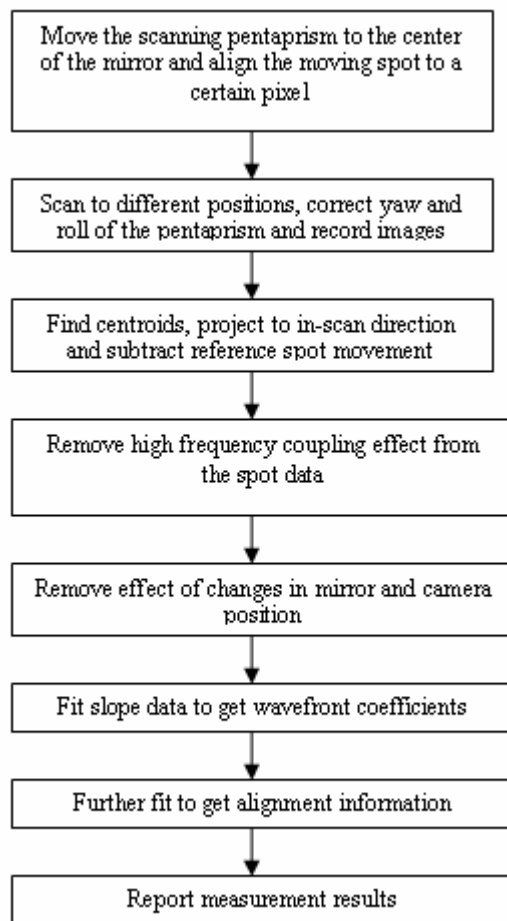

Fig. 5. Flow diagram for data collection and processing

3.3 Result of the NST test

Four scans were taken to get a measurement of the surface figure. After several iterations of measuring and adjusting the alignment, the pentaprism assembly was well-aligned to the mirror. Thirty-seven points were sampled during each scan. At each scanning position, five spot images were recorded and averaged. Fig.6 shows the spot diagrams obtained from the four scans. The spot diagrams have been corrected based on high-frequency data from the interferometric measurement. Fig. 7 shows the polynomial fitting result, and Fig. 8 shows the residuals after removing the field aberrations and the polynomial fit to figure errors. The focal length is 3.85 m, so a wavefront slope error of 1 μrad corresponds to 3.85 μm of spot motion.
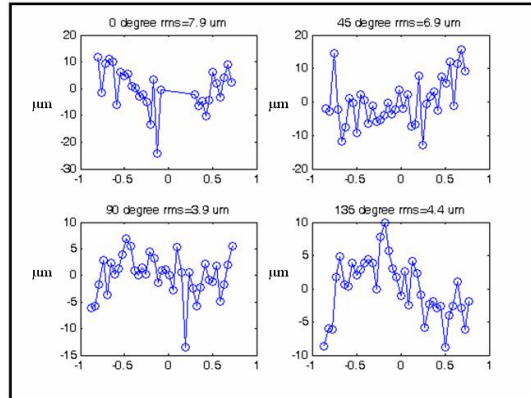

Fig. 6. In-scan spot displacements after subtracting motion of the reference spot, and the effects of small-scale figure errors
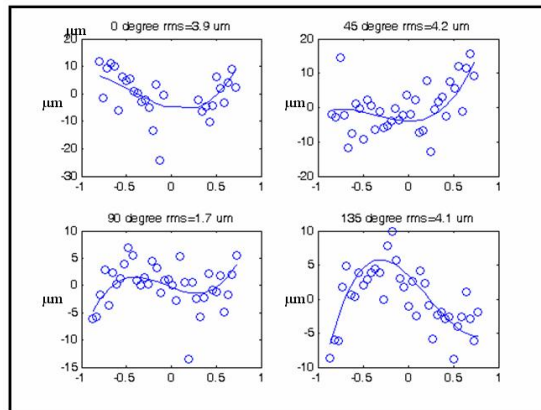

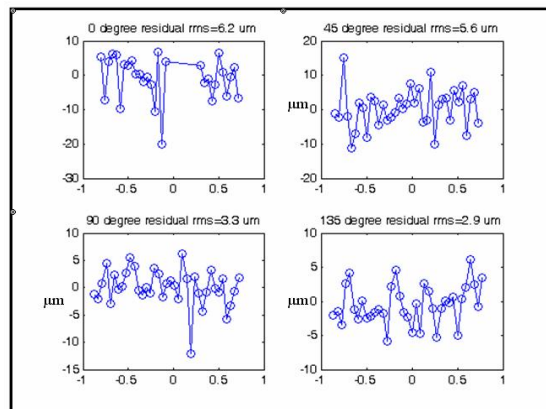Fig. 7. Fit of Zernike polynomials to the spot displacements

Fig.8. Residuals after removing the polynomial fit and field aberrations

We also measured the figure of the NST mirror with a full-aperture interferometric test. Both measurements were made during the figuring process, before the mirror was finished. The mirror was in the same state for both measurements. The optical test is made from the mirror's center of curvature, with a single-element diffractive null corrector. Alignment tolerances for the interferometer and hologram are very tight, leading to significant uncertainty in low-order aberrations. We needed the pentaprism measurement in order to verify the accuracy of measurement for these aberrations. Fig. 9 shows the surface measurements from both tests, and Table 2 lists the coefficients of the fit from the pentaprism test and coefficients obtained from an interferometric null test. The two measurements agree within the expected uncertainties of the pentaprism test, which are estimated as described in the next section.
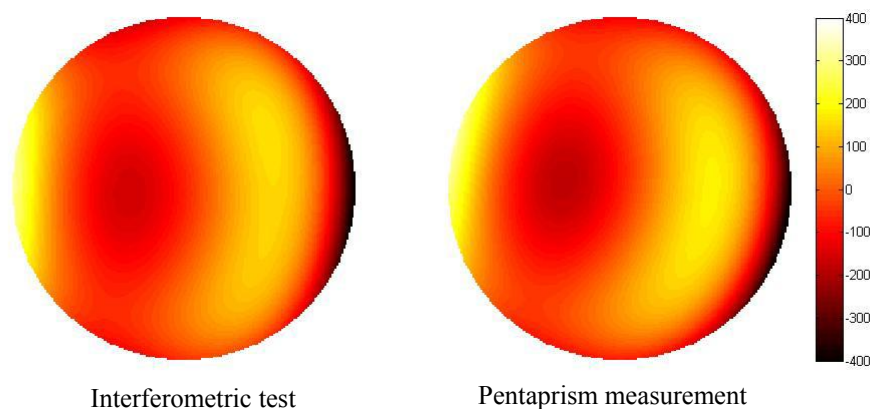

Fig. 9. Surface estimate from the pentaprism test and an interferometric test. Color bar is labeled in nm of surface error.

Table 2. Surface coefficients from pentaprism test and interferometric test

aberration	interferometer	pentaprism
	nm rms surface	nm rms surface
astigmatism 0°	8	9 ± 23
astigmatism 45°	0	-2 ± 23
coma 0°	-87	-98 ± 12
coma 90°	-4	16 ± 12
trefoil 0°	-50	-32 ± 35
trefoil 30°	9	23 ± 35
spherical	-32	-35 ± 8

3.4 Error analysis

3.4.1 Effect of errors

We calculated the effect of 1 µrad random errors in wavefront slope with a Monte Carlo analysis. Results are shown in Table 3 for both the NST mirror and the GMT segment. In the NST measurement, some points near the edge of the mirror could not be sampled due to the configuration of the pentaprism test. This causes the estimated uncertainty to be larger than the situation where the full aperture is sampled. The GMT measurement will have more nearly uniform sampling because the components are smaller relative to the mirror and the system is designed to minimize obscuration. While the analysis in the table assumes four scans as in the NST measurement, the GMT pentaprism system will allow additional scans in order to achieve better sensitivity to trefoil.

Table 3. Monte Carlo analysis of 1 μrad rms random error in wavefront slope

aberration	rms surface error (nm) Sampled as in NST measurement	rms surface error (nm) Sampled uniformly, for NST mirror (40 points/scan)	rms surface error (nm) Sampled uniformly, for GMT segment (4 scans, 40 points/scan)
Focus	15	9	44
Sine Astigmatism	23	17	84
Cosine Astigmatism	23	17	84
Sine Coma	12	6	30
Cosine Coma	12	6	30
Sine Trefoil	35	20	99
Cosine Trefoil	35	20	99
Spherical aberration	8	4	20
RSS	**58**	**36**	**180**

3.4.2. Spot position error

We use a correlation method to find the positions of the spots in the focal plane. We record the intensity distribution of a "master spot" by averaging a large number of frames. For each measured spot, we find the position of the master spot that gives the maximum correlation. We have found this method to be more immune to noise than a simple centroid calculation. We estimate an uncertainty of 1.5 μm rms in this determination. For the difference between the stationary and scanning pentaprisms, an uncertainty of 2.1 μm rms ($\sqrt{2} \times 1.5$) is expected. This is equivalent to 0.55 μrad rms wavefront slope error.

3.4.3. Errors from motions and misalignment

Errors in angular motions and alignment have only second-order effects on the measured slopes. Table 4 lists the degrees of freedom of the sources of errors. Table 5 gives a summary of the error terms that couple to the measurement. These sources of error combine as shown in Table 1 to produce a wavefront slope error estimated at 0.26 μrad rms.

Table 4. Sources of error due to angular motions and misalignment

	Pitch	**Yaw**	**Roll**
Beam projector	Yes	Yes	No
Prism	No	Yes	Yes
Focal plane	No	No	Yes

3.4.4. Other error sources

In addition to the errors due to misalignment of components described in the previous section, there are errors related to variations in field angle, motion of the detector, and wavefront errors in the collimated beam and the pentaprisms. These are described briefly below and in more detail in Reference 5.

Table 5. Estimates of alignment errors for the NST pentaprism system

Parameter	Description	Estimated error in this parameter
Beam projector pitch	Directly couples to the slope measurement. Removed by using differential motion between stationary and scanning pentaprisms.	~0.03mrad rms
Δ(beam projector yaw)	Variation in beam projector line of sight in yaw direction	<0.4mrad rms
Prism yaw	Misalignment of prism in yaw direction due to initial alignment	<0.02mrad rms
Δ(Prism yaw)	Variation of yaw orientation for prism	<0.1mrad rms
Prism roll	Roll changes were removed with feedback from the spot motion on the detector.	~0.4mrad
Detector roll	Determination of the in-scan direction on the detector	~0.5mrad

3.4.4.1 Error due to field and focus variation between scans

During the test, the pentaprism assembly was aligned to the same field angle for all scans. This was done by focusing the light to the same pixel on the detector for the central point of the scan, which is common to all scans. In addition, the relative position changes between the mirror and the detector were monitored by a laser tracker and compensated numerically in the data reduction process.

We estimate that residual field variations were at the level of ±1.6 µrad. We performed a Monte-Carlo analysis to determine the effect on the measured aberrations. It is insignificant at 2.2 nm rms surface error. The laser tracker measurements indicate that a ±3 µm focus uncertainty may exist, which corresponds to a 7.1 nm rms surface error.

3.4.4.2. Error due to beam projector pitch

Due to the field aberrations, a variation in beam projector pitch has slightly different effects on the spots from the stationary and scanning pentaprisms. We simulated this effect and developed correction factors, and these factors were verified by changing the pitch of the rail and measuring the difference in motion between the two spots.

3.4.4.3. Wavefront errors coupled with lateral motion of prisms

Phase or amplitude variations in the collimated beam from the beam projector do not affect the system performance to first order because these effects are common to both prisms. However, these variations are coupled with lateral motion of the prism assembly relative to the collimated beam. In the NST measurement, a stop was set at the scanning prism so that the same portion of the prism was used at all times. This was done because the prism has larger errors (due to index inhomogeneity and surface aberrations) than the beam.

Three basic couplings with lateral motion of the prism have been identified and analyzed:[6]

1. Coupling of phase errors in the collimated beam with lateral motion of the prism.

2. Coupling of diffraction effects in the collimated beam with lateral motion of the prism .

3. Coupling of amplitude variations in the collimated beam with lateral motion of the prism.

These three effects give a change of slope that will be proportional to the lateral motion of the scanning pentaprism. The lateral motion of the prisms is likely to be systematic, with low-order dependence on scan position. The most troublesome error terms come from lateral motion that varies linearly and quadratically with scan position. A linear variation is interpreted as focus or astigmatism, while a quadratic variation is interpreted as coma and a cubic variation as spherical aberration. The analysis shows that these errors can be made insignificant (<0.3 µrad rms wavefront slope) by limiting the systematic lateral motion of the prism to <2 mm, limiting slope errors at the edge of the collimated beam to 3 µrad, making the stop on the scanning pentaprism at least 10% smaller than any previous stop, and keeping the intensity of the collimated beam uniform to 20%.

3.4.5. Summary of the errors

Taking account of all error sources, the uncertainty of the NST pentaprism test is estimated to be 50 nm rms surface.

4. SUMMARY

We have developed a scanning pentaprism test and applied it to measure an off-axis surface for which field aberrations can be significant. Field aberrations introduce a number of new sources of error and issues that complicate the data acquisition and reduction. These issues are now understood mathematically and resolved experimentally in the measurement of the NST mirror. The scanning pentaprism test is an important verification test for the GMT segments. The NST measurements demonstrate that the test can be made to work at a level consistent with the predicted performance.

5. ACKNOWLEDGEMENT

6. REFERENCES

[1] Burge, J. H., *Advanced Techniques for Measuring Primary Mirrors for Astronomical Telescopes*, Ph. D. Dissertation, Optical Sciences, University of Arizona (1993).
[2] Yellowhair, Julius, Peng Su, Robert Sprowl, Robert Stone, Jim Burge, "Development of a 1 meter vibration insensitive Fizeau interferometer, " to be submitted to Optical Express (2008).
[3] Burge, J. H., L. B. Kot, H. M. Martin, C. Zhao, T. Zobrist, "Alternate surface measurements for GMT primary mirror segments, " Optomechanical Technologies for Astronomy, edited by Eli Atad-Ettedgui, Joseph Antebi, Dietrich Lemke, Proc. of SPIE Vol. 6273, 62732T (2006).
[4] Burge, J. H., L. B. Kot, H. M. Martin, R. Zehnder, C. Zhao, "Design and analysis for interferometric measurements of the GMT primary mirror segments, " Optomechanical Technologies for Astronomy, edited by Eli Atad-Ettedgui, Joseph Antebi, Dietrich Lemke, Proc. of SPIE Vol. 6273, 62730M (2006).
[5] Peng Su, James H. Burge, Brian Cuerden, Hubert M. Martin, "Scanning Pentaprism Measurements of Off-axis Aspherics," to be submitted to Applied Optics.
[6] Mallik, Proteep C. V., Chunyu Zhao, James H. Burge, "Measurement of a 2-meter flat using a pentaprism scanning system," Optical Engineering 46(2), 023602 (2007).